



Contents lists available at ScienceDirect

Journal of King Saud University – Science

journal homepage: [www.sciencedirect.com](http://www.sciencedirect.com)

Original article

# Green and chemical synthesis of CuO nanoparticles: A comparative study for several *in vitro* bioactivities and *in vivo* toxicity in zebrafish embryos

Sabeena G<sup>a</sup>, Rajadurai S<sup>b</sup>, Pushpalakshmi E<sup>a</sup>, Hisham A. Alhadlaq<sup>c</sup>, Raja Mohan<sup>d</sup>, Annadurai G<sup>a,\*</sup>, Maqsood Ahamed<sup>c,\*</sup><sup>a</sup> Sri Paramakalyani Centre of Excellence in Environmental Sciences, Manonmaniam Sundaranar University, Alwarkurichi 627412, India<sup>b</sup> Sri Paramakalyani College, Manonmaniam Sundaranar University, Alwarkurichi 627412, India<sup>c</sup> Department of Physics and Astronomy, College of Science, King Saud University, Riyadh 11451, Saudi Arabia<sup>d</sup> Chemical Industry Research Institution, University of Ulsan, Ulsan 44776, South Korea

## ARTICLE INFO

### Article history:

Received 10 March 2022

Revised 31 March 2022

Accepted 11 May 2022

Available online 17 May 2022

### Keywords:

CuO NPs

Green vs. chemical methods

Zebrafish

Cytotoxicity

Antibacterial activity

Antidiabetic activity

Anti-inflammatory activity

## ABSTRACT

CuO NPs is being applied for various applications including catalyst, electronics, cosmetics, and biomedicines due to its exceptional physicochemical properties. Physical and chemical routes for CuO NPs synthesis raised the concern of environmental hazard due to use of high energy, high temperature, and toxic chemicals. Conversely, green procedure is considered as an inexpensive and eco-friendly approach. To compare *in vitro* bioactivities and *in vivo* toxicity, CuO NPs was synthesized by two different methods; green and chemical routes. Leaf extract of a medicinal plant (*Salacia reticulata*) was used as a reducing and capping agent for green synthesis of CuO NPs. Sodium hydroxide was applied for chemical route of CuO NPs preparation. The *in vivo* toxicity of both CuO NPs (green and chemical) was examined in zebrafish (*Dania rerio*) embryos. Several *in vitro* biological activities e.g. antibacterial, cytotoxicity (in human cells), antidiabetic, and anti-inflammatory activities of both CuO NPs (green and chemical) was also assessed. Prepared CuO NPs (green and chemical) was characterized by SEM-EDX, FTIR, XRD, and UV–Vis spectroscopy. Several biomarkers such as hatching rate, malformation, and mortality rate of zebrafish embryos showed that green prepared CuO NPs exerted much lesser toxicity as compared to chemically synthesized CuO NPs. Antibacterial activity of green CuO NPs against Gram-negative (*Escherichia coli*, *Staphylococcus aureus*, and *Enterobacter*) and Gram-positive (*Bacillus subtilis* and *Pseudomonas aeruginosa*) bacteria was higher than chemical CuO NPs. Cytotoxicity results showed that human breast cancer cells (MCF-7) were more sensitive to green CuO NPs than chemical CuO NPs. Furthermore, antidiabetic and anti-inflammatory activities of green CuO NPs was greater than those of chemically prepared CuO NPs. This work revealed that *in vitro* bioactivities of green synthesized CuO NPs was better than chemically synthesized CuO NPs. Green CuO NPs also displayed higher biocompatibility towards zebrafish than chemical CuO NPs. This work highlights the importance eco-friendly green synthesis of CuO NPs for biomedical applications.

© 2022 The Author(s). Published by Elsevier B.V. on behalf of King Saud University. This is an open access article under the CC BY-NC-ND license (<http://creativecommons.org/licenses/by-nc-nd/4.0/>).

\* Corresponding authors.

E-mail addresses: [gannadurai@msuniv.ac.in](mailto:gannadurai@msuniv.ac.in) (A. G.), [mahamed@ksu.edu.sa](mailto:mahamed@ksu.edu.sa) (M. Ahamed).

Peer review under responsibility of King Saud University.



## 1. Introduction

The creation of nanoscale materials is expanding consistently due to their diverse applications from aerospace, agriculture, to biomedical and bioengineering (Ahamed et al., 2021). It is likewise realized that the particles and molecules of metals or non-metals in nanoscale range display extraordinary characteristics in comparison to their parent bulky materials (Ahamed et al., 2015). There are several physical, chemical, and green routes for the synthesis of nanoscale materials (Noorjahan et al., 2015). Physical and chemical methods of nanoparticles (NPs) synthesis are not advisable for

<https://doi.org/10.1016/j.jksus.2022.102092>

1018-3647/© 2022 The Author(s). Published by Elsevier B.V. on behalf of King Saud University.

This is an open access article under the CC BY-NC-ND license (<http://creativecommons.org/licenses/by-nc-nd/4.0/>).

their application in biomedical fields due to the use of high energy, high temperature, and toxic chemicals (Ahamed et al., 2022a). Green synthesis of NPs is an inexpensive and eco-friendly process that does not require toxic chemicals (Ahamed et al., 2022b). In green route, biological compounds such as sugar, polyphenols, alkaloids, and phenolic acids are utilized as a reducing and capping agent for reduction of metal ions into NPs in a very controlled way (Kuppusamy et al., 2016). Utilization of harmless biological compounds in green procedure is now providing a better option for synthesis of various types NPs for biomedical and clinical applications.

The *Salacia reticulata* has been employed in traditional medicine for treatment and prevention various disorders including asthma, amenorrhea, and dysmenorrhea (Morikawa et al., 2021). Besides, water extracts of leaves of *Salacia reticulata* has also shown potential for the prevention of diabetes and obesity as its multiple effects such as the ability to increase the plasma insulin level and lower the lipid peroxide level of the kidney (Yoshino et al., 2009). *Salacia reticulata* leaves contain several phytochemicals that can be utilized in green synthesis of various NPs. However, information on application *Salacia reticulata* in the synthesis of bio-medically relevant NPs is largely lacking.

CuO NPs has been shown potential for diverse application such as catalyst, battery, gas-sensor, heat transfer fluid, electronics, and cosmetics because of its superior physicochemical properties (Shah and Lu, 2018). CuO NPs is also found to be utilized in various biomedical applications including antimicrobial, biosensor, and cancer therapy (Ahamed et al., 2014; Siddiqui et al., 2013). In terms of healing, activation of pro- and anti-inflammatory pathways are important for the enlargement of protective strategies to shield the regenerative tissue from damage caused by imbalances in cytokines, oxidants, and antioxidants (Kenneth et al., 2009). Role of NPs in antidiabetic activity is one of the thrust areas of nanotechnology as it was estimated that by the year 2030, diabetes mellitus affected population will rise up to 366 million worldwide (Dhiraj et al., 2019).

There is limited information on comparative bioactivity/toxicity of green and chemically prepared CuO NPs. This study was designed to examine the comparative biological activity (*in vitro*) and toxicity (*in vivo*) of CuO NPs prepared by two different routes; green and chemical methods. Leaves extract of *Salacia reticulata* was applied as a reducing and capping agent for green synthesis of CuO NPs, while sodium hydroxide was used for chemical synthesis of CuO NPs. Prepared samples were characterized by UV-vis spectrophotometer, FTIR, XRD, and SEM-EDX techniques. The *in vitro* bioactivities such as antidiabetic, anti-inflammatory, cytotoxicity, and antibacterial activity of both CuO NPs (green and chemical) was assessed. Comparative toxicity of both types CuO NPs was also explored in zebrafish (*Dania rerio*) embryos. The zebrafish model represents a feasible alternate to the mammalian prototypes presently used in toxicity testing and other biological studies. Zebrafish are easier and less expensive to house and care for as compared to rodent models (Garcia, et al., 2016; Kumari et al., 2017).

## 2. Experimental plan

### 2.1. Preparation of leaf extract

Copper nitrate ( $\text{CuN}_2\text{O}_6 \cdot 3\text{H}_2\text{O}$ ), polyvinylpyrrolidone (PVP), and sodium hydroxide (NaOH) was purchased from Organic Trading (Pvt) Ltd (Colombo, Sri Lanka). The *Salacia reticulata* leaves were obtained from department of agriculture, eastern university, Sri Lanka (EUSL). The *Salacia reticulata* leaves were washed thoroughly with distilled water and cut into small pieces. The 10 g of *Salacia*

*reticulata* leaves pieces were transferred to 80 mL of distilled water and boiled for 20 min. Then, solution was filtered to obtain extract. The leaf extract was stored at 4 °C until further use.

### 2.2. Green synthesis of CuO NPs

Fig. 1 shows green route CuO NPs preparation. In brief, 3 mL of leaf extract was added to 40 mL of aqueous copper nitrate solution (1 mM) in a 250 mL flask. This solution was incubated for 24 h at 4 °C. A change in color from blue to green suggested the formation of colloidal suspension of CuO NPs. Colloidal suspension was further dried at 120 °C for 2 h to get the CuO NPs powder.

### 2.3. Chemical synthesis of CuO NPs

Fig. 2 represents chemical route of CuO NPs synthesis. The initial precursors were copper nitrate, NaOH, and PVP. Briefly, PVP and copper nitrate (0.1 M) was dissolved in 50 mL distilled water. Then, aqueous solution of NaOH (0.5 M) added dropwise to above solution and stirred for 30 min to complete the precipitation process. Precipitate was washed several times and dried at 120 °C for 2 h. Finally, precipitate was calcined at 500 °C for 4 h to get powder of CuO NPs.



Fig. 1. Green synthesis of CuO NPs.

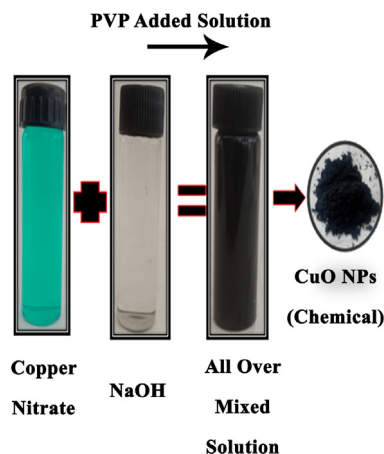


Fig. 2. Chemical synthesis of CuO NPs.

### 2.4. Characterization of prepared samples

Optical absorption was recorded at UV-Vis spectrophotometer. FTIR was performed in the range of 500–4000  $\text{cm}^{-1}$ . Crystallinity and phase purity was examined by X-Ray diffraction. Morphology was assessed scanning electron microscopy (SEM).

### 2.5. Zebrafish maintenance and their breeding to embryos

Zebrafish (*Dania rerio*) were maintained in wealth section loaded up with the adapted water (75 g  $\text{NaHCO}_3$ , 18 g ocean salt, 8.4 g  $\text{CaSO}_4$ , per 1000 L). We housed wild-type adult zebrafish (*Dania rerio*) (Aquatic Environments) in an independent framework (Aquatic Habitats), maintained and bred zebrafish as reported earlier (Browning et al., 2009). In brief, two pairs of mature zebrafish placed into a clean incubator and applied a light (14 h)-dark (10 h) cycle to trigger fertilization and breeding of embryos. Eggs were gathered into a petri dish and washed multiple times with E3 medium.

### 2.6. Embryos toxicity study

The test is predominantly founded on the incipient organism test system created by Schulte and Nagel (1994). Briefly, 100 eggs were placed into a 96-well multi-plates with 10 eggs for every well. Then, each was loaded with E3 medium containing CuO NPs (green and chemical). Well without NPs (only E3 medium) serves as a control. The 96-well plate was covered with the plastic film and set in an enlightenment hatchery at  $28 \pm 1^\circ\text{C}$  with a light (14 h)-dark (10 h) cycle. The immediate perception was acted in the well under a light magnifying instrument associated with a camera gadget at indicated time focuses (24, 48, 72, and 96 hpf). The toxicological endpoints included mortality, gastrula improvement, tail separation, eyes, somite arrangement, circulatory framework, heartbeat, pigmentation, otic container, bring forth rate, distortions, and length of hatchlings were recorded. After 96 hpf exposure, the chorion was thoroughly taken out from the

unhatched eggs with little youngsters. The hatchlings were situated on the parallel side and shot. The length of hatchlings was estimated utilizing advanced picture investigation (Scion Picture, ver. 4.0.3.2.). The half bring hatching rate (HT50) was determined utilizing Sigmoid Fit by Beginning 8.0 (Beginning Lab, US).

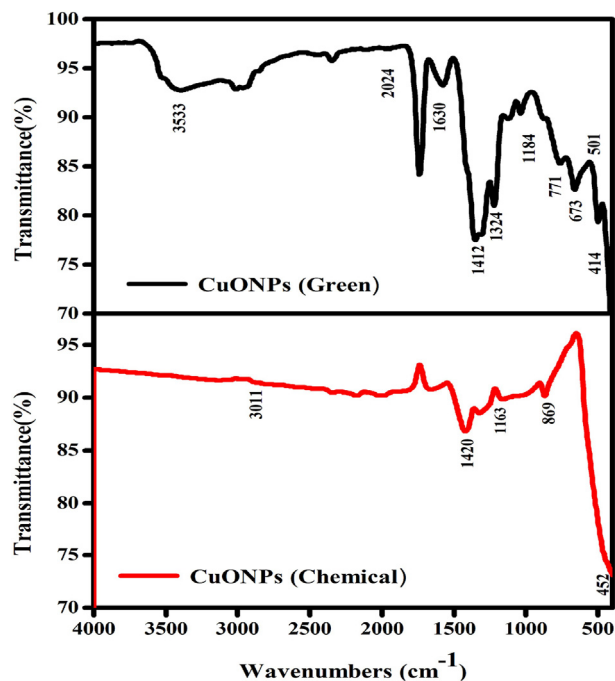


Fig. 4. The FTIR spectar CuO NPs (Chemical and Green).

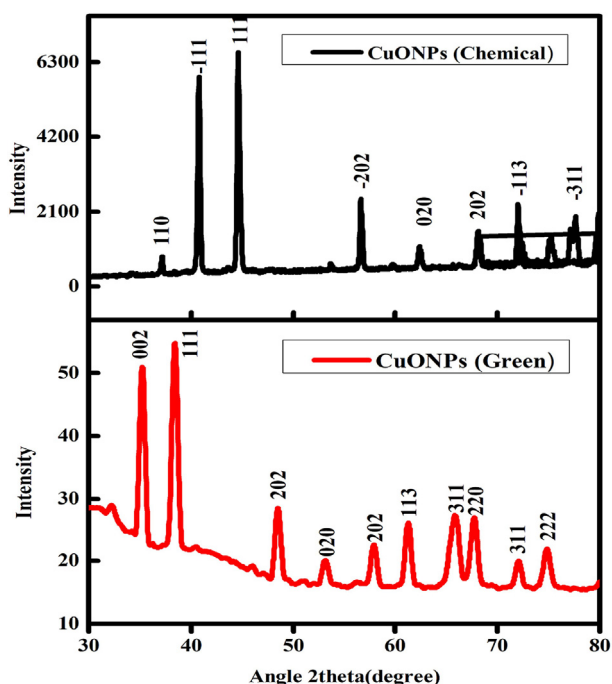


Fig. 3. XRD spectra of CuO NPs (Chemical and Green).

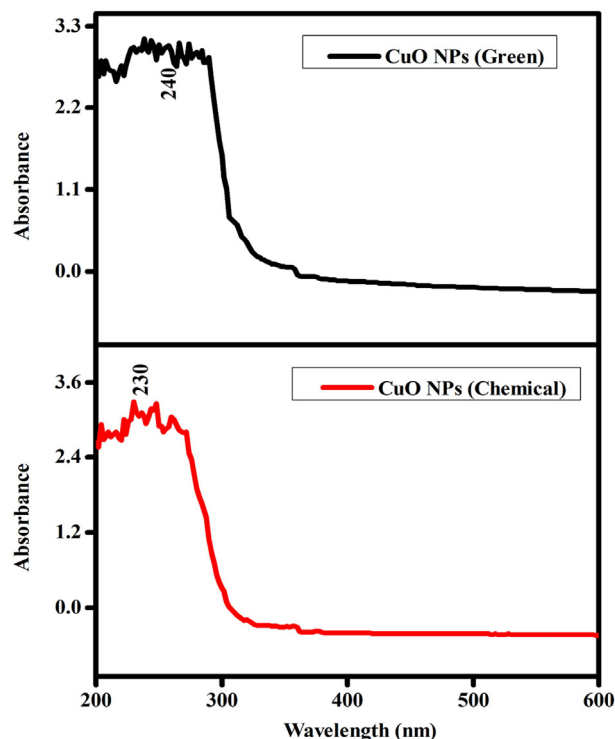


Fig. 5. UV-visible absorbance CuO NPs (Green and Chemical).

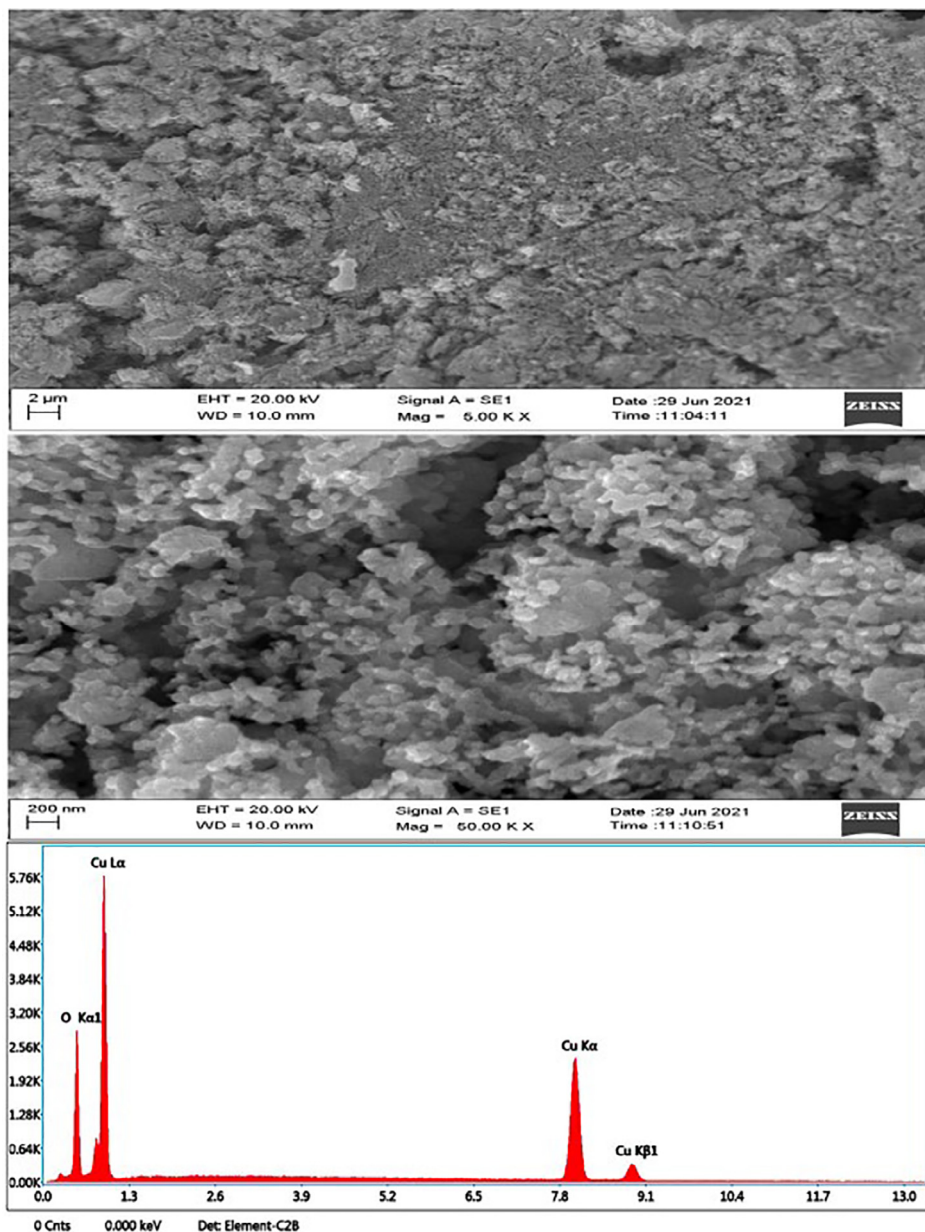


Fig. 6a. SEM-EDX study of CuO NPs (Green).

### 2.7. Antidiabetic assay

The  $\alpha$ -glucosidase inhibition assay was performed as reported earlier (Butala et al., 2018). For this assay, 10–50  $\mu$ l/mL of the test samples (CuO NPs) were aliquoted into 96-well plates and diluted with 0.02 M sodium phosphate buffer (pH 6.9). Then 50  $\mu$ l of  $\alpha$ -glucosidase was added to above mixture. Further, 50  $\mu$ l of p-nitrophenyl- glucoopyranoside (pNPG) (3 mM) was mixed as a substrate and reaction solutions further incubated for 20 min at 37 °C. Next, 50  $\mu$ l of  $\text{Na}_2\text{CO}_3$  (0.1 M) was added to reach the reaction at stationary phase. Absorbance was documented at 405 nm wavelength through a microplate reader.

### 2.8. Anti-inflammatory activity

The diclofenac sodium was used as a standard reagent for denaturation of bovine serum albumin (BSA). Both CuO NPs (green and chemical) were used for inhibitions of BSA denaturation process to test the scavenging activity as described earlier (Gunathilake et al., 2018). CuO NPs was dissolved in dimethylformamide (DMF) and diluted with 0.2 M of phosphate buffer (pH 7.4). The obtained DMF concentration in all the solutions was maintained by <2.5%. The 4 mL containing the NPs with the different concentrations (10–50  $\mu$ l/ml) was mixed in 1 mL of BSA (1 mM) incubated for 15 min at 37 °C and then heated to 51 °C

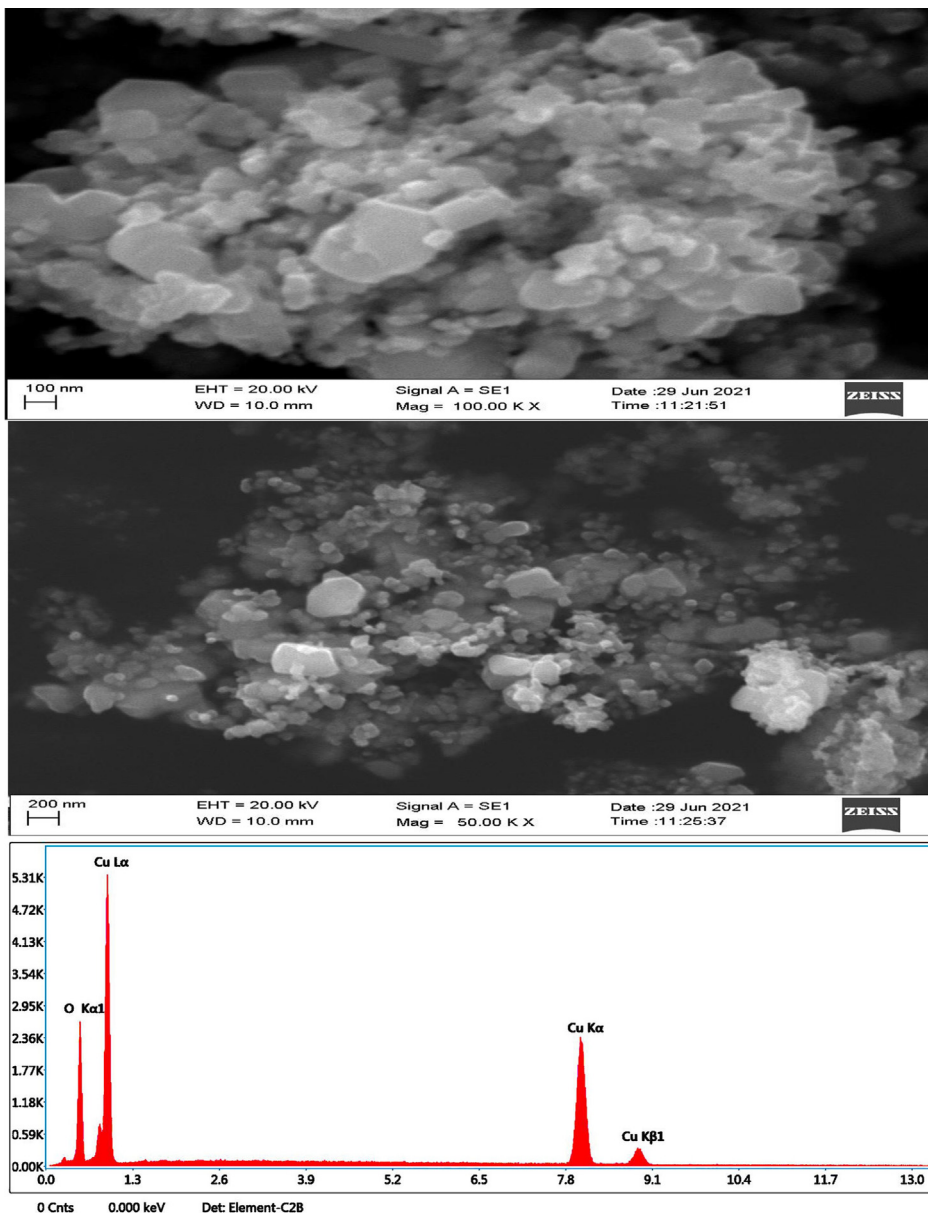


Fig. 6b. SEM-EDX study CuO NPs (Chemical).

for 20 min. After cooling samples to room temperature the turbidity was estimated at 660 nm by UV–vis spectrophotometer.

2.9. Cytotoxicity assay

MTT assay was used to evaluate the cytotoxicity of CuO NPs (green and chemical) in human keratinocytes (HaCaT) and human breast cancer cells (MCF-7) (Ahamed et al., 2019). Both cell lines were obtained from National Centre for Cell Sciences (NCCS, Pune,

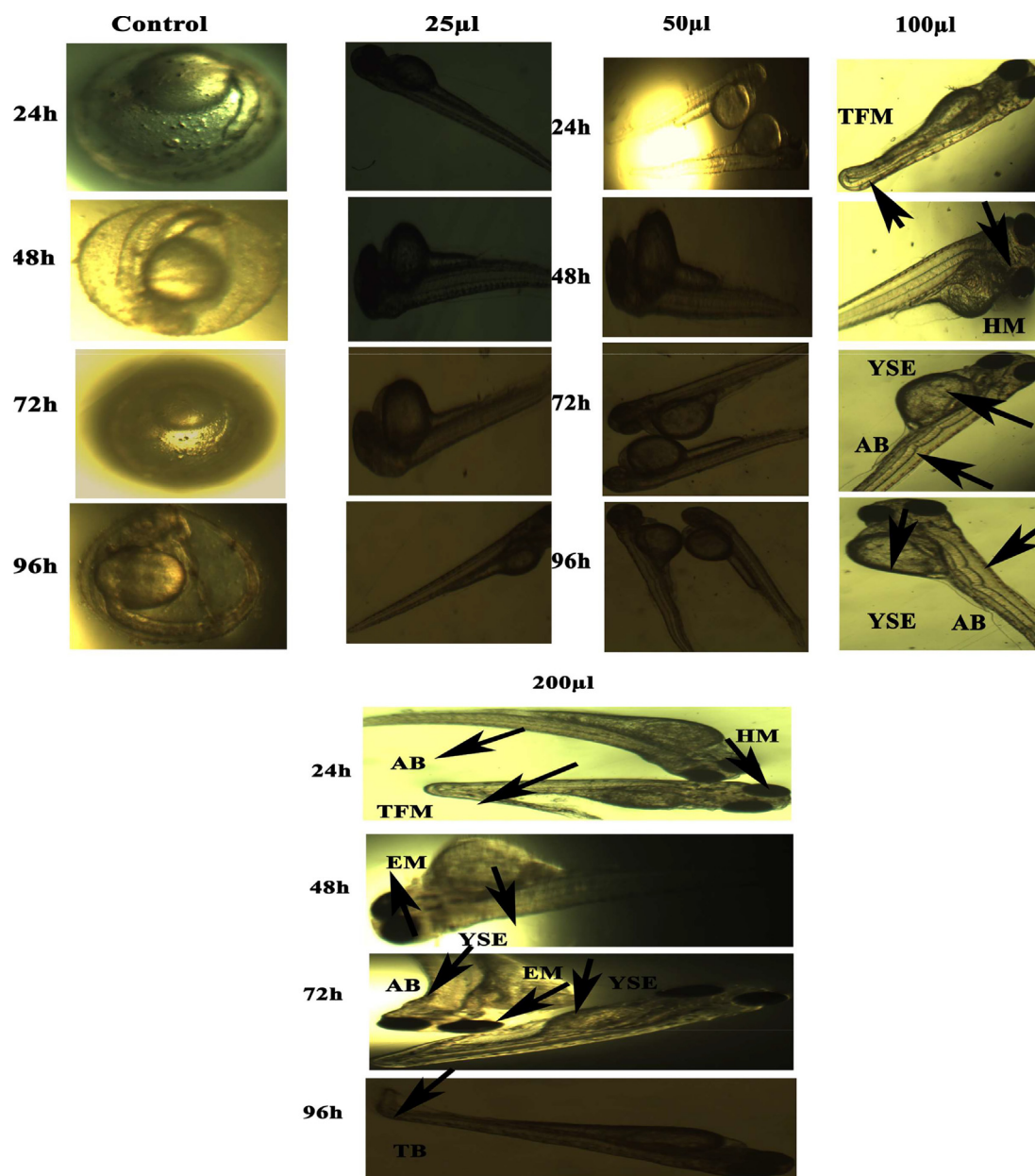
India). Cells ( $1 \times 10^5$  cells/mL) were cultured in 96-well plates with Dulbecco’s modified Eagle medium (DMEM) containing 10% FBS and 1% penicillin/streptomycin. Cells were allowed to attach the surface for 24 h at 37 °C with 5% CO<sub>2</sub> supply. Cells were then treated for 24 h with various concentrations of NPs (0.1, 0.5, 1, 5, 10, 50, and 100 µg/mL). After exposure, 0.5 mg/mL of MTT added to each well and incubated for 4 h at 37 °C. Metabolically active cells formed formazan crystals, which were dissolved in SDS. The absorbance of solution was recorded 570 nm using an ELISA reader.

Table 1a  
Elemental composition of CuO NPs (Green).

S.No	Element	Weight %	Atomic %
1	O K	17.8	46.2
2	CuK	82.2	53.8

Table 1b  
Elemental composition of CuO NPs (Chemical).

S.No	Element	Weight %	Atomic %
1	O K	17.2	45.2
2	CuK	82.8	54.8



**Fig. 7a.** Representative images of zebrafish embryos and larvae exposed to CuO NPs (Green). The control group shows the normal appearance at 24 hpf, 48 hpf, 72 hpf, and 96 hpf. Tail bent (TB), yolk sac edema (YSE), head malformation (HM), axis bent (AB) and & tail fold malformation (TFM) denoted the malformation after exposure to 100–200  $\mu$ l of CuO NPs (Green) for 48–96 hpf.

### 2.10. Antibacterial activity

Both gram-negative (*Escherichia coli*, *Staphylococcus aureus*, and *Enterobacter*) and gram-positive (*Bacillus subtilis* and *Pseudomonas aeruginosa*) bacterial strains were applied to test the antibacterial potential of prepared samples. These bacterial strains were received from Microbial Type Culture Collection and Gene Bank (MTCC), Institute of Microbial Technology, Chandigarh, India. Both types of bacterial strain were maintained in the nutrient agar medium at 37 °C. Antibacterial activity of *Salacia reticulata* leaf extract and CuO NPs (green and chemical) were analysed utilizing a standard agar well dispersion strategy (Mulvaney, 1996). The Muller Hinton agar containing the microbial inoculum was spread everywhere on the Petri plate. Permit it to cool for quite a while, and afterward a well of distance across 8–10 mm was punched aseptically with a sterile cork borer or a tip. Different concentrations of NPs and extract was added into the well, and agar plates were

incubated under sterile conditions. The NPs diffused into the agar media and restrain the development of organisms. At that point, the antibacterial movement of the nanoparticles was distinguished by the presence of the restraint zone around the agar well.

## 3. Results and discussion

### 3.1. X-ray diffraction study

XRD spectra of CuO NPs (green and chemical) is presented in Fig. 3. The estimated particle size for CuONPs (chemical) was around 84 nm, while CuONPs (green) size was around 42.2 nm. Sharp peaks indicating the crystalline nature of both prepared samples. The XRD patterns of NPs produced chemically and biologically match the reference patterns for CuO NPs in the available literature (Premana and Yulizar, 2017; Nagabhushana et al., 2016).

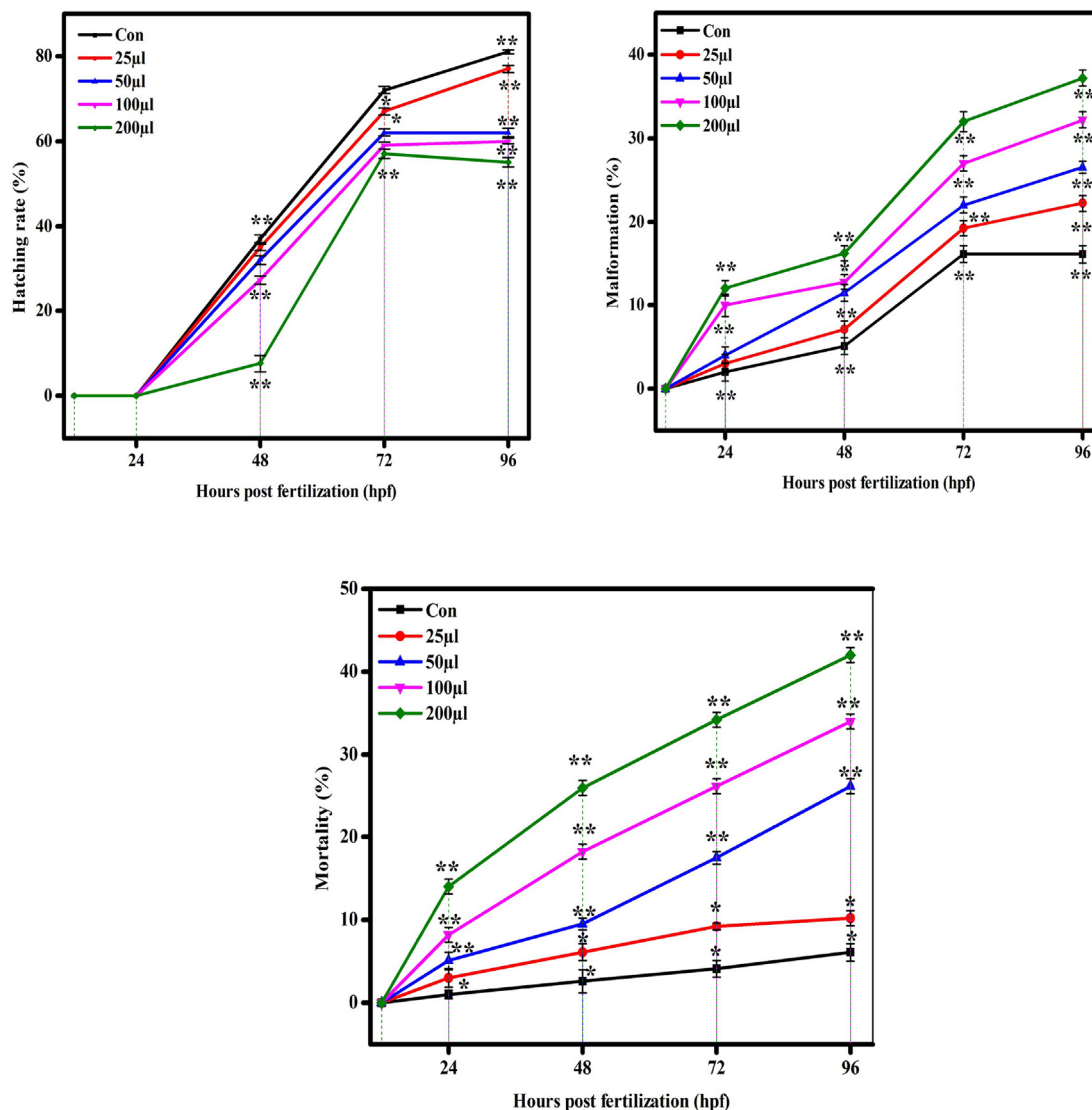


**Fig. 7b.** Hatching, malformation, and mortality rate in zebrafish against CuO NPs (Green). The data are presented as mean  $\pm$  SD of three experiments. The data were analysed statistically by one way analysis of variance (ANOVA) followed by Dunnett's Multiple range test (Tukey's post-hoc test) using GraphPad Prism software. Significance "" and """" represent  $p < 0.05$  and  $p < 0.01$ , respectively.

XRD spectra illustrates that the strength and quality of XRD peaks vary based on the methods of preparation (green vs. chemical).

### 3.2. FTIR study

FTIR analysis was done to perceive the possible biomolecules that are accountable for the creation of CuO NPs. Fig. 4 represents the FTIR spectra of CuO NPs (green and chemical) was recorded in the range of 500–4000  $\text{cm}^{-1}$ . FTIR spectra of both samples show a smooth comparable curvature with slight difference. The broad peak observed at 3533  $\text{cm}^{-1}$  corresponds to the O–H and N–H bond stretching vibrations. The vibrations might be appropriate to phenolic compounds in attendance in the solution (Mamun et al., 2017). The minute peak at 2024  $\text{cm}^{-1}$  correspond to the stretching vibrations of the compounds containing  $\text{C}\equiv\text{N}$  bonds. The sharp peak at 1630  $\text{cm}^{-1}$  corresponds to the presence of  $\text{C}=\text{N}$  or  $\text{C}=\text{O}$  stretching. Likely, peak at 1412  $\text{cm}^{-1}$  indicate  $\text{sp}^3$  C–H bending or acyl C–O (or phenol C–O) stretching and

1324  $\text{cm}^{-1}$  denotes C–H stretching. Additionally, peak at 1184  $\text{cm}^{-1}$  denotes alkoxy C–O. The unsaturated C–H bending appears under 771  $\text{cm}^{-1}$  that might be due to the presence of bioactive phytochemicals. These compounds might impart capping which helps in maintaining the stability of CuO NPs. Moreover, a sharp peak found in the infrared spectrum at low frequencies at 673–414  $\text{cm}^{-1}$  corresponds to CuO vibrations which were in accordance with earlier reports (Kumari et al., 2017). CuO NPs (green) bands around 1420  $\text{cm}^{-1}$  and 1163  $\text{cm}^{-1}$  are due to the characteristic frequency of inorganic ions. CuO NPs (chemical) displayed prominent peaks at 3011  $\text{cm}^{-1}$ , 1420  $\text{cm}^{-1}$ , 1163  $\text{cm}^{-1}$ , 869  $\text{cm}^{-1}$ , 452  $\text{cm}^{-1}$ . A strong intensity band at 1,058  $\text{cm}^{-1}$  may be due to S–O–C stretching. The stretching vibrations assigned to the C–S linkage occur in the region of 800–600  $\text{cm}^{-1}$  and the weak S–S stretching vibration falls between 600 and 400  $\text{cm}^{-1}$  (Upadhyay et al., 2020). A comparative strong peak was observed CuO NPs (green) synthesized broad peak at 1184  $\text{cm}^{-1}$  and CuO NPs (chemical) synthesized broad peak 1163  $\text{cm}^{-1}$  is due to C–O stretching of the capping (Nasrullah et al., 2020).

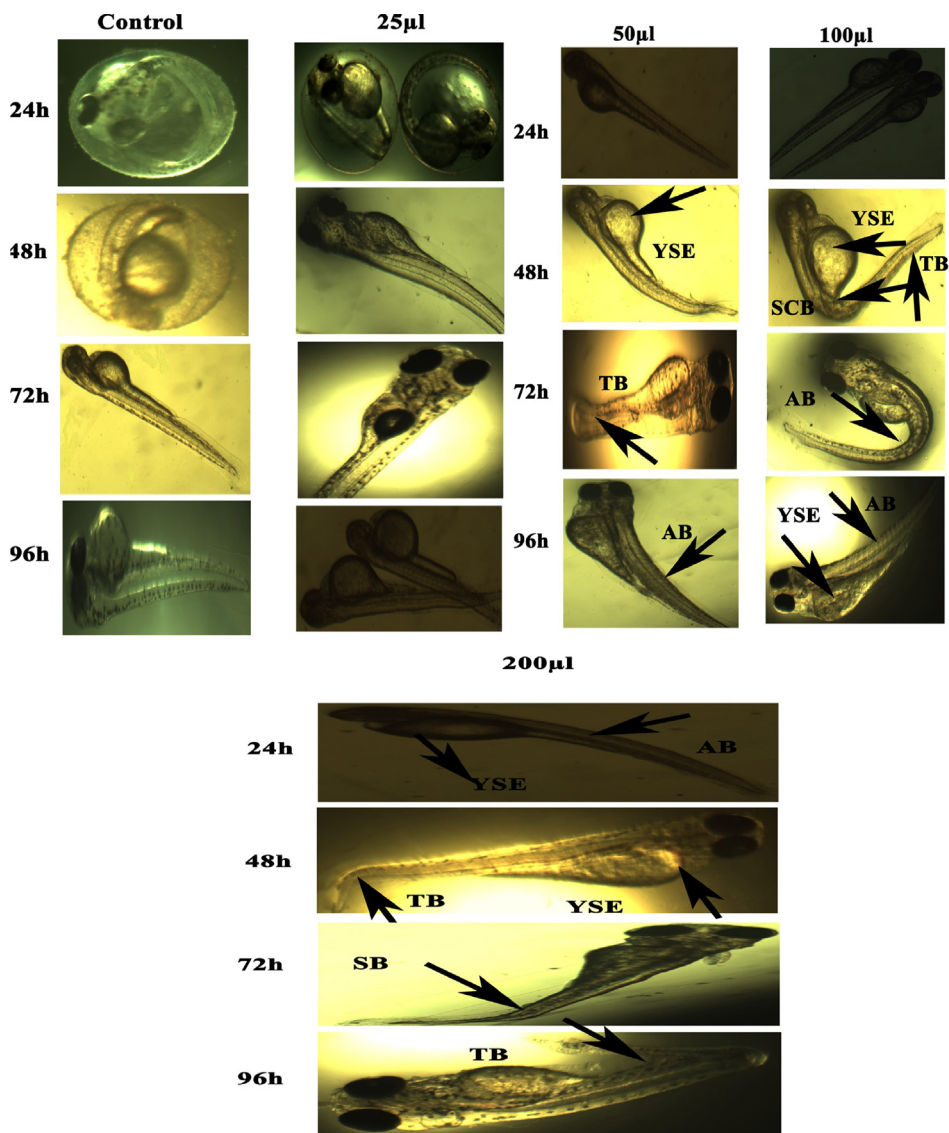


**Fig. 8a.** Representative images of zebrafish embryos and larvae exposed to CuO NPs (Chemical). The control group shows the normal appearance at 24 hpf, 48 hpf, 72 hpf, and 96 hpf. Tail bent (TB), yolk sac edema (YSE), head malformation (HM), axis bent (AB) and tail fold malformation (TFM) denoted the malformation after exposure to 100–200 µl of CuO NPs (Chemical) for 48–96 hpf.

### 3.3. UV–vis spectroscopy

Fig. 5 represents the UV–visible absorption spectra of both CuO NPs (green and chemical) with slight shifting of absorption peak. In green synthesis, a change in color from blue to green of colloidal suspension suggests the formation of CuO NPs. Hence, the absorption peak for the green synthesized CuO NPs was recorded at 240 nm. In chemical route color of solution changed from colourless to black. As a consequences of UV–visible absorption peak for the chemically prepared CuO NPs was observed at 230 nm.

### 3.4. SEM-EDX study

Morphology of prepared CuO NPs (chemical and green) was investigated by SEM-EDX (Figs. 6a and b). These images suggested that CuO NPs prepared by green method was more dispersed than chemically prepared CuO NPs. This could be due to adsorption phytochemical on the surface of NPs during green synthesis. Size calculated from SEM images for both types of NPS (green and chemical) were in agreement with size recorded from XRD data.

As seen from the SEM images, green CuO NPs has much lower particle size than chemical CuO NPs. The change in size was due to presence natural capping agent during green preparation (Upadhyay et al., 2020). EDX spectra showed that Cu and O were main elements in prepared CuO NPs (green and chemical). Tables 1a and b represent elemental composition of CuO NPs (green and chemical). These results were in agreement with previous studies (Sukumar et al., 2020). Fig. 7a. Fig. 7b. Fig. 8a. Fig. 8b..

### 3.5. Toxicity study in zebrafish embryos and larvae

There are several reports demonstrated the toxicity of metal and metal oxide NPs in zebrafish embryos (Asharani et al., 2008; Zhu et al., 2008). Physicochemical characteristics e.g. shape, size, and surface area are responsible factors for toxicity of metal oxide NPs in zebrafish embryos. Figures 7 (a and b) and 8 (a and b) show the comparative toxicity of CuO NPs (green vs. chemical). Large amount of CuO NPs (green and chemical) deposited on egg surfaces. The mortality of zebrafish eggs and larvae exposed to various concentrations (25, 50, 100, 200 µl/ml) of CuO NPs (green and

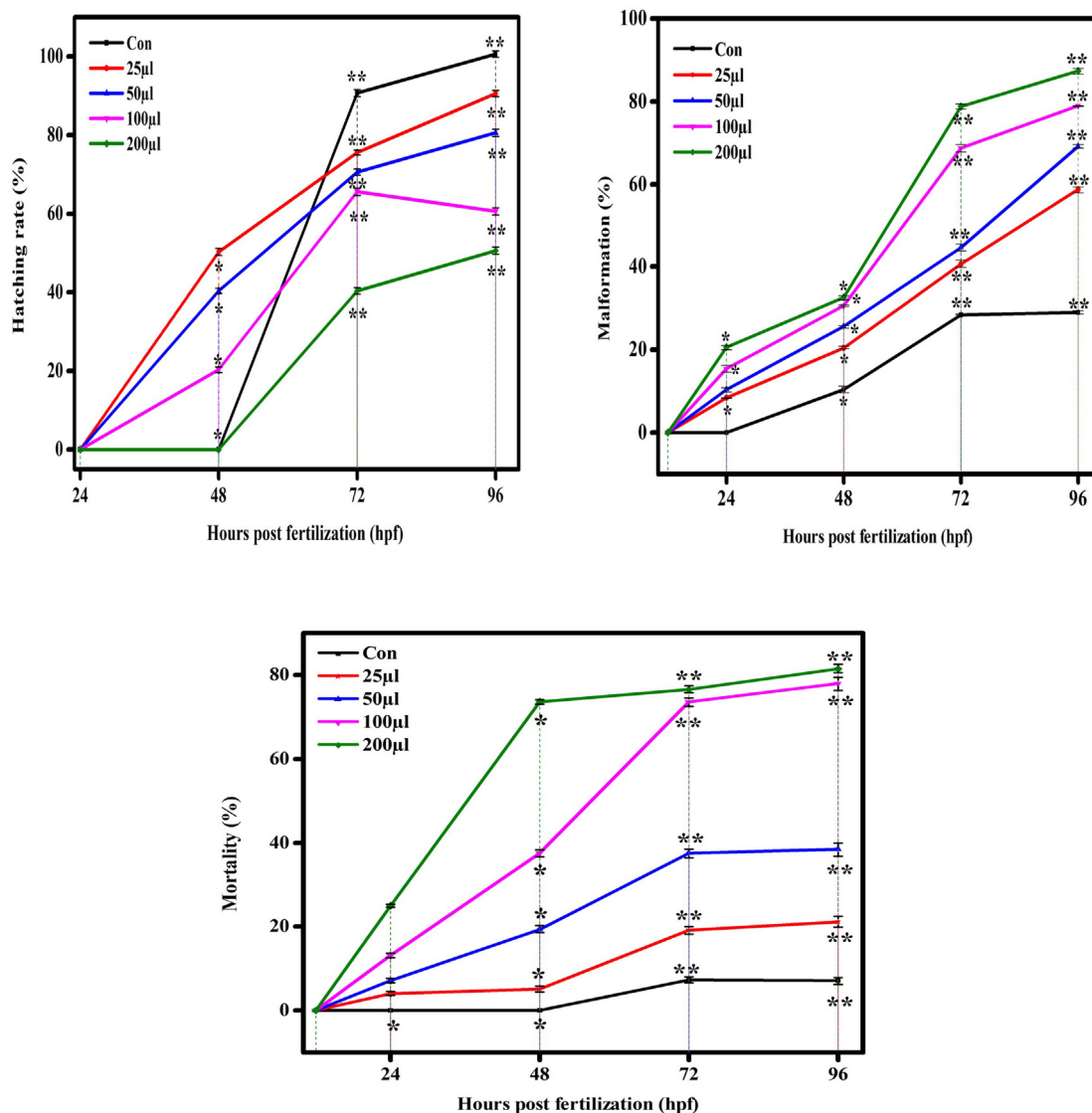


**Fig. 8b.** Hatching, malformation, and mortality rate in zebrafish against CuO NPs (Chemical). The data are presented as mean ± SD deviation of three experiments. The data were analysed statistically by one way analysis of variance (ANOVA) followed by Dunnett's Multiple range test (Tukey's post-hoc test) using GraphPad Prism software. Significance "\*" and "\*\*" represent  $p < 0.05$  and  $p < 0.01$ , respectively.

**Table 2**  
Comparison of touch responses of CuO NPs (Green vs. Chemical).

Concentration µl/ml	Touch and Swim Response		Legend
	CuO NPs (Green)	CuO NPs (Chemical)	
Control	++++	++++	++++ Fast response
25	++++	+++	+++ Medium response
50	++++	++	++ Slow response
100	++++	+	+ Very Slow response
200	+++	-	- No response

chemical) was evaluated for certain time periods. At 200 µl/ml, CuO NPs exhibited significant anomalies. As shown in Figures 7 and 8, exposure to CuO NPs (green and chemical) disturbed the development embryos characterized by several malformations e.g. spinal card bent (SB), yolk sac edoema (YSE), tail bent (TB), head malformation (HM), axis bent (AB), eye malformation (EM), tail fold malformation (TFM), and delayed hatching rate at higher concentrations (100 and 200 µl/ml) for 24–96 hpf. CuO NPs also

displayed significant killing of zebrafish embryos. Table 2 also shows the comparison of touch responses of embryos after exposure to CuO NPs (green vs. chemical). These results demonstrated that green CuO NPs produce much less toxicity to zebrafish than chemical CuO NPs. Earlier studies also reported the such malformations in zebrafish embryos after exposure to CuO NPs, ZnO NPs, ZrO NPs, and SiO<sub>2</sub> NPs (Bai et al., 2010, Duan et al., 2013, Ganesan et al., 2016).

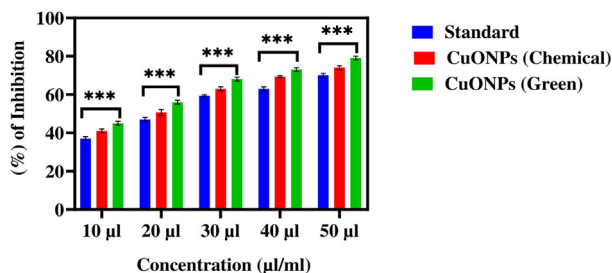


**Fig. 9.** The  $\alpha$ -glucosidase inhibition activity of CuO NPs (Green and Chemical). The data are presented as mean  $\pm$  SD of three replications. The data were analysed statistically by Two-way analysis of variance (ANOVA) followed by Dunnett's multiple range test (Tukey's post-hoc test) using GraphPad Prism Software. Bars labeled with "\*\*\*\*" represent statistically significant results ( $p < 0.001$ ).

**Table 3**

IC<sub>50</sub> values of antidiabetic activity, anti-inflammatory activity, and cytotoxicity.

Assays	Parameters/ cell lines	IC <sub>50</sub> value ( $\mu$ L)- Standard	IC <sub>50</sub> value ( $\mu$ L)- CuO NPs (Chemical)	IC <sub>50</sub> value ( $\mu$ L)- CuO NPs (Green)
<b>Antidiabetic Activity</b>	$\alpha$ -glucosidase assay	29	26	22
<b>Anti-inflammatory Activity</b>	BSA denaturation	267	274	109
<b>Cytotoxicity</b>	HaCaT cells	0.4	0.3	0.6
	MCF-7 cells	0.3	0.36	0.42

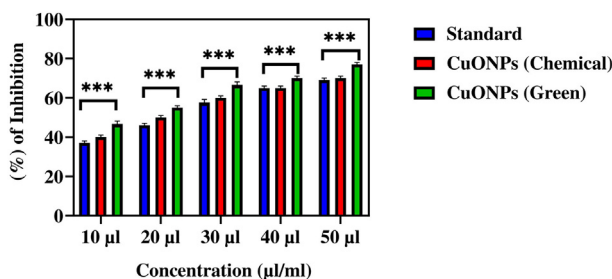


**Fig. 10.** Percentage of bovine serum albumin (BSA) inhibition activity of CuO NPs (Green and Chemical). The data are presented as mean  $\pm$  SD of three replications. The data were analysed statistically by Two-way analysis of variance (ANOVA) followed by Dunnett's multiple range test (Tukey's post-hoc test) using GraphPad Prism Software. Bars labeled with "\*\*\*\*" represent statistically significant results ( $p < 0.001$ ).

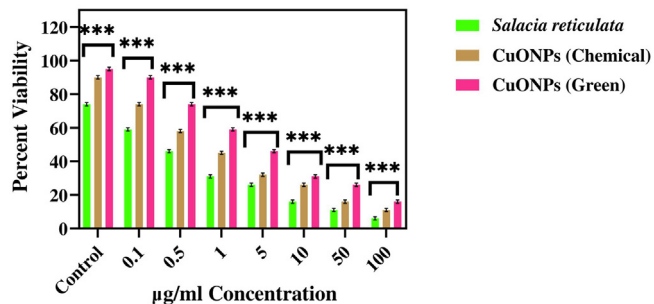


**Fig. 11a.** Cytotoxicity assay in normal human keratinocyte (HaCaT) cells after the treatment with several concentrations of CuO NPs (Green and Chemical) and leaf extract of *Salacia reticulata*. Data represent mean  $\pm$  SD of three replications. The data were analysed statistically by two-way analysis of (ANOVA) followed by Dunnett's multiple range test (Tukey's post-hoc test) using GraphPad Prism Software. Bars labeled with "\*\*\*\*" represent statistically significant results ( $p < 0.001$ ).

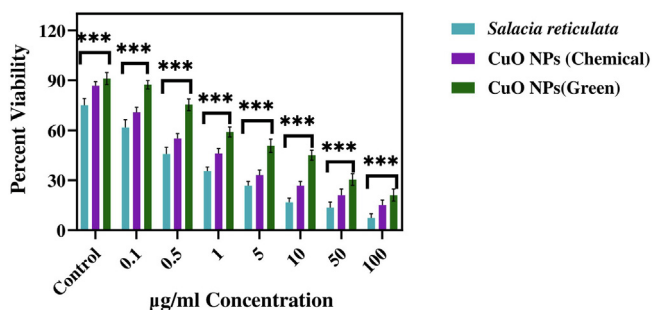


**Fig. 11b.** Cytotoxicity assay in human breast cancer (MCF-7) cells after the treatment with several concentrations of CuO NPs (Green and Chemical) and leaf extract of *Salacia reticulata*. Data represent mean  $\pm$  SD of three replications. The data were analysed statistically by two-way analysis of (ANOVA) followed by Dunnett's multiple range test (Tukey's post-hoc test) using GraphPad Prism Software. Bars labeled with "\*\*\*\*" represent statistically significant results ( $p < 0.001$ ).

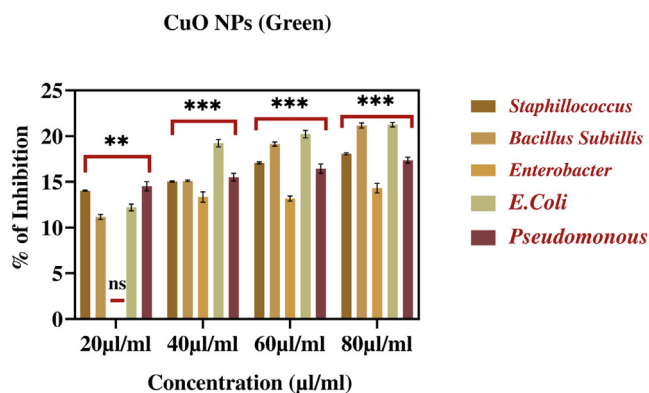


**Fig. 12a.** Percentage inhibition of bacterial growth against CuO NPs (Green). The data are presented as mean  $\pm$  SD of three replications. The data were analysed statistically by Two-way analysis of variance (ANOVA) followed by Dunnett's multiple range test (Tukey's post-hoc test) using GraphPad Prism software. Significance "\*\*\*\*" represent  $p < 0.01$ , "ns" represent No Significance. Bars labelled with "\*\*\*\*" represent statistically significant results  $p < 0.001$ .

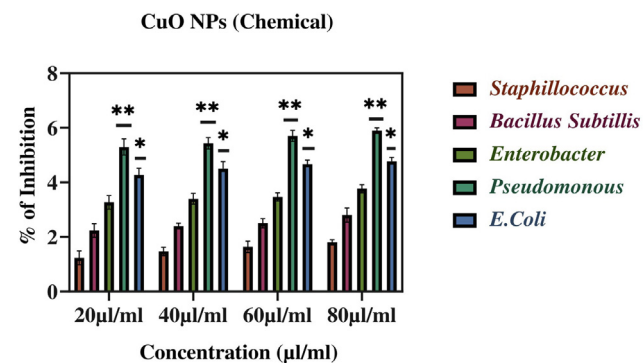


**Fig. 12b.** Percentage inhibition of bacterial growth against CuO NPs (Chemical). The data are presented as mean  $\pm$  SD of three replications. The data were analysed statistically by Two-way analysis of variance (ANOVA) followed by Dunnett's multiple range test (Tukey's post-hoc test) using GraphPad Prism software. Significance "\*\*\*\*" and "\*\*\*\*" represent  $p < 0.05$  and  $p < 0.01$ .

### 3.6. Antidiabetic activity

To reduce hyperglycaemia therapeutically, carbohydrate-digesting enzymes such as  $\alpha$ -glucosidase must be inhibited to prevent the breakdown of carbohydrates into monosaccharides that are major contributor in high sugar level in the blood (Exteberria

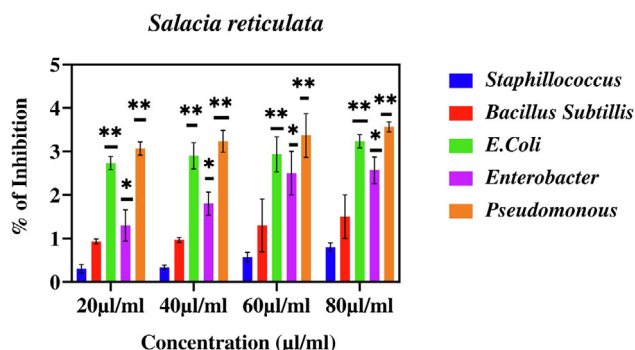


**Fig. 12c.** Percentage inhibition of bacterial growth against leaf extract of *Salacia reticulata*. The data are presented as mean ± SD of three replications. The data were analysed statistically by Two-way analysis of variance (ANOVA) followed by Dunnett’s multiple range test (Tukey’s post-hoc test) using GraphPad Prism software. Statistically Significance “\*\*” and “\*\*\*\*” represent p < 0.05 and p < 0.01.

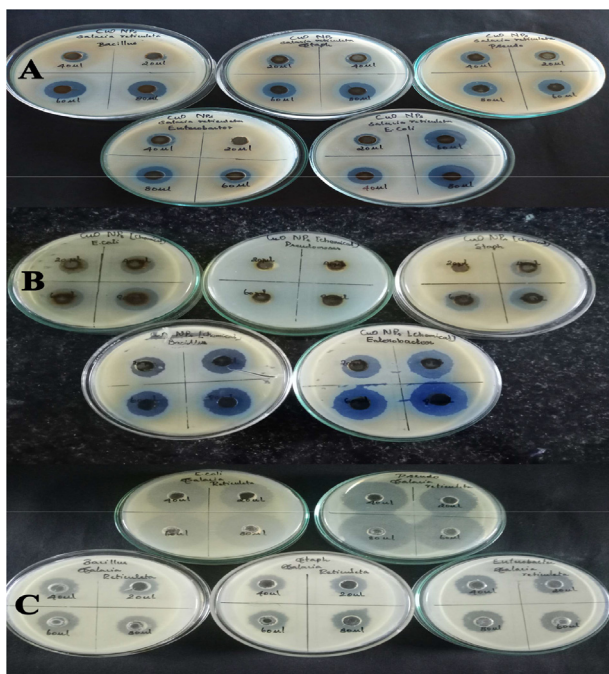


**Fig. 13.** Zone of inhibition assay. (A) CuO NPs-Green. (B) CuO NPs-Chemical. (C) Leaf extract of *Salacia reticulata*.

**Table 4**

Antibacterial activity of CuO NPs (Green and Chemical) and leaf extract of *Salacia Reticuleta* against several pathogenic bacteria.

Sample	Bacteria	20 µl/ml	40 µl/ml	60 µl/ml	80 µl/ml
CuO NPs (Green)	<i>Staphylococcus</i>	14.03 ± 0.05	15.03 ± 0.05	17.03 ± 0.1	18.06 ± 0.1
	<i>Bacillus</i>	11.1 ± 0.2	15.1 ± 0.1	19.1 ± 0.2	21.1 ± 0.2
	<i>Enterobacter</i>	0	13.3 ± 0.5	13.1 ± 0.2	14.3 ± 0.5
	<i>E.Coli</i>	12.2 ± 0.3	19.2 ± 0.4	20.2 ± 0.4	21.2 ± 0.2
	<i>Pseudomonous</i>	14.5 ± 0.5	15.5 ± 0.43	16.4 ± 0.5	17.3 ± 0.3
CuO NPs (Chemical)	<i>Staphylococcus</i>	1.2 ± 0.2	1.4 ± 0.1	1.6 ± 0.2	1.8 ± 0.1
	<i>Bacillus</i>	2.2 ± 0.2	2.4 ± 0.1	2.5 ± 0.17	2.8 ± 0.26
	<i>Enterobacter</i>	3.26 ± 0.25	3.4 ± 0.2	3.46 ± 0.15	3.7 ± 0.15
	<i>E.Coli</i>	4.26 ± 0.25	4.5 ± 0.2	4.6 ± 0.15	4.7 ± 0.15
	<i>Pseudomonous</i>	5.3 ± 0.3	5.4 ± 0.2	5.7 ± 0.2	5.9 ± 0.1
<i>Salacia reticulata</i>	<i>Staphylococcus</i>	0.3 ± 0.1	0.33 ± 0.05	0.5 ± 0.1	0.8 ± 0.1
	<i>Bacillus</i>	0.93 ± 0.05	0.96 ± 0.05	1.3 ± 0.6	1.5 ± 0.5
	<i>Enterobacter</i>	1.3 ± 0.3	1.8 ± 0.26	2.5 ± 0.5	2.56 ± 0.3
	<i>E.Coli</i>	2.7 ± 0.1	2.9 ± 0.3	2.93 ± 0.40	3.2 ± 0.1
	<i>Pseudomonous</i>	3.0 ± 0.1	3.2 ± 0.2	3.3 ± 0.5	3.5 ± 0.1

et al., 2012). In this study, antidiabetic activity ( $\alpha$ -glucosidase inhibition assay) of CuO NPs (green and chemical) is presented in Fig. 9. Results showed that both types of CuO NPs (green and chemical) induce dose-dependent inhibition of  $\alpha$ -glucosidase enzyme activity in the concentration range of 10–50 µl/mL. The IC<sub>50</sub> values of antidiabetic activity for green and chemical CuO NPs was 22 µl/mL and 26 µl/mL, respectively (Table 3). Moreover, antidiabetic activity of green CuO NPs was slightly higher than chemically produced CuO NPs. Hence, green prepared CuO NPs has potential to be further studied for the treatment of diabetes.

### 3.7. Anti-inflammatory activity

Anti-inflammatory activity of CuO NPs (green and chemical) was measured using bovine serum albumin (BSA) denaturation assay. Different concentrations (10–50 µg/mL) of both CuO NPs was applied for anti-inflammatory assay. Results showed that both CuO NPs exhibit anti-inflammatory activity in a dose-dependent manner (Fig. 10). Similarly, a recent study observed that the anti-inflammatory activity of CuO NPs using the BSA denaturation approach (Gnanasundaram and Balakrishnan, 2017). Another study also reported the anti-inflammatory activity of Ag NPs (Prabakaran and Mani, 2019). The IC<sub>50</sub> values of anti-inflammatory activity for chemical and green CuO NPs was 274 µl/mL and 109 µl/mL, respectively (Table 3). This data suggested that green prepared CuO NPs is a better agent in creation of active medicines for inflammatory diseases.

### 3.8. Cytotoxicity study

MTT assay is a widely accepted method to study the cytotoxicity of metal oxide NPs (Ahamed et al., 2021). In the present work, the cytotoxicity of leaf extract (*Salacia reticulata*) and CuO NPs (Chemical and Green) was assessed in human keratinocyte (HaCaT) and human breast cancer (MCF-7) cells (Figs. 11a and b). Cells were exposed to different concentrations of leaf extract and CuO NPs (0.1–100 µg/mL) for 24 h. Results showed that leaf extract both types of CuO NPs decreased the viability of two cells in a dose-dependent manner. The IC<sub>50</sub> value of both types of CuO NPs (green and chemical) for HaCaT and MCF-7 cells is given presented in Table 3. These results suggested that green synthesized CuO NPs exert higher cytotoxicity towards MCF-7 cancer cells than those of CuO NPs prepared by chemical method.

Results of the present study are in agreement with several previous reports. Our earlier study reported that CuO NPs induced cytotoxicity in human liver cancer (HepG2) cells in a concentration

dependent manner. (Siddiqui et al., 2013). Different metal NPs, metal oxide NPs and metal oxide-based nanocomposites prepared by chemical and green methods also demonstrated anticancer activity against several types of human cancer cells (Ahamed et al., 2021a, 2021b, 2022a, 2022b). In this study, we did not explore the potential mechanisms of anticancer activity of prepared samples. Role of oxidative stress in anticancer activity of NPs is actively being investigated. However, exact mechanisms of anticancer potential of nanoscale materials still remains a daunting task.

### 3.9. Antibacterial efficacy

Percentage of inhibition of bacterial growth due to leaf extract and CuO NPs (green and chemical) is presented in Figs. 12a–c. These figures suggested that CuO NPs display excellent antibacterial activity against both gram-positive and gram-negative bacteria. Zone of inhibition images provided in Fig. 13 that also indicates the potential inhibition against bacterial pathogens by tested materials. These results suggested the dose-dependent antibacterial activity of leaf extract and CuO NPs (green and chemical) (Table 4).

Moreover, green prepared CuO NPs shown better antibacterial activity against *Bacillus* and *E. Coli* when compared to other three pathogenic bacteria (Fig. 13). Importantly, green produced CuO NPs demonstrated substantial antibacterial activity against both gram-positive and gram-negative bacterial pathogens. Our results are supported by previous findings of antibacterial activity of different types of NPs (Ahamed et al., 2014; Jain and Mehata, 2017; Rautela et al., 2019; Rokade et al., 2016).

## 4. Conclusions

In summary, CuO NPs was produced by two different methods; chemical and green routes. Several *in vitro* biological activities and *in vivo* toxicity in zebrafish was examined against both types of CuO NPs (green and chemical). Results showed that green prepared CuO NPs exhibits higher antidiabetic and anti-inflammatory activity than those of chemically synthesized CuO NPs. Antibacterial activity of green CuO NPs against gram-positive and gram-negative bacterial pathogens was higher in comparison to CuO NPs produced by chemical method. Human breast cancer cells (MCF-7) displayed greater vulnerability against green CuO NPs than those of chemical CuO NPs. Interestingly, green CuO NPs exhibited less toxicity to zebrafish embryos than chemically synthesized CuO NPs. This study offers an inexpensive and eco-friendly approach for green synthesis CuO NPs with the potential of its application in pharmaceutical industries.

## 5. Ethics approval

All the animal experiments were carried out in compliance with the standard ethical guidelines and under the control of the Sri Paramakalyani Centre for Excellence in Environmental Science–Manonmaniam Sundaranar University of Animal Ethics Committee.

## Declaration of Competing Interest

The authors declare that they have no known competing financial interests or personal relationships that could have appeared to influence the work reported in this paper.

## Acknowledgement

The authors extend their sincere appreciation to the Researchers Supporting Project (RSP-2021/129) at the King Saud University, Riyadh, Saudi Arabia.

## References

- Ahamed, M., Akhtar, M.J., Khan, M.A.M., Alrokayan, S.A., Alhadlaq, H.A., 2019. Oxidative stress mediated cytotoxicity and apoptosis response of bismuth oxide (Bi<sub>2</sub>O<sub>3</sub>) nanoparticles in human breast cancer (MCF-7) cells. *Chemosphere* 216, 823–831. <https://doi.org/10.1016/j.chemosphere.2018.10.214>.
- Ahamed, M., Akhtar, M.J., Khan, M.A.M., Alhadlaq, H.A., 2022a. Enhanced anticancer performance of eco-friendly-prepared Mo-ZnO/RGO nanocomposites: Role of oxidative stress and apoptosis. *ACS Omega* 7 (8), 7103–7115. <https://doi.org/10.1021/acsomega.1c06789>.
- Ahamed, M., Akhtar, M.J., Khan, M.A.M., Alhadlaq, H.A., 2021a. SnO<sub>2</sub>-doped ZnO/reduced graphene oxide nanocomposites: synthesis, characterization, and improved anticancer activity via oxidative stress pathway. *Int. J. Nanomedicine* 16, 89–104. <https://doi.org/10.2147/IJN.S285392>.
- Ahamed, M., Akhtar, M.J., Alhadlaq, H.A., Alrokayan, S.A., 2015. Assessment of the lung toxicity of copper oxide nanoparticles: Current status. *Nanomedicine (Lond.)* 10 (15), 2365–2377. <https://doi.org/10.2217/nmm.15.72>.
- Ahamed, M., Alhadlaq, H.A., Khan M.A.M., Karuppiah, P., Al-Dhabi, N.A., 2014. Synthesis, characterization and antimicrobial activity of copper oxide nanoparticles. *J. Nanomater.* 2014, 637858. <https://doi.org/10.1155/2014/637858>.
- Ahamed, M., Akhtar, M.J., Khan, M.A.M., Alhadlaq, H.A., 2022b. Facile green synthesis of ZnO-RGO nanocomposites with enhanced anticancer efficacy. *Methods* 199, 28–36. <https://doi.org/10.1016/j.jymeth.2021.04.020>.
- Ahamed, M., Akhtar, M.J., Khan, M.A.M., Alhadlaq, H.A., 2021b. A novel green preparation of Ag/RGO nanocomposites with highly effective anticancer performance. *Polymers* 13 (19), 3350. <https://doi.org/10.3390/polym13193350>.
- Asharani, P.V., Lian Wu, Y.I., Gong, Z., Valiyaveetil, S., 2008. Toxicity of silver nanoparticles in zebrafish models. *Nanotechnology*. 19 (25). <https://doi.org/10.1088/0957-4484/19/25/255102>.
- Bai, W., Zhang, Z., Tian, W., He, X., Ma, Y., Zhao, Y., Chai, Z., 2010. Toxicity of zinc oxide nanoparticles to zebrafish embryo: a physicochemical study of toxicity mechanism. *J. Nanopart. Res.* 12 (5), 1645–1654.
- Browning, L.M., Lee, K.J., Huang, T., Nallathambiy, P.D., Lowman, J.E., Nancy, X.H., 2009. Random walk of single gold nanoparticles in zebrafish embryos leading to stochastic toxic effects on embryonic developments. *Nanoscale*. 1, 138. <https://doi.org/10.1039/b9nr00053d>.
- Butala, M.A., Kukkupuni, S.K., Venkatasubramanian, P., Vishnuprasad, C.N., 2018. An ayurvedic anti-diabetic formulation made from curcuma longa L. and Emblica officinalis L. Inhibits  $\alpha$ -amylase,  $\alpha$ -glucosidase, and starch digestion, *in vitro*. *Starch* 70, 1700182. <https://doi.org/10.1002/star.201700182>.
- Dhiraj, A., Jamdade., Dishantsingh., R., Komal., A., Joshi., Rohini, K., 2019. Gnidia glauca- and plumbago zeylanica-mediated synthesis of novel copper nanoparticles as promising antidiabetic agents. *Adv. Pharmacol. Sci.* 2019, 9080279. <https://doi.org/10.1155/2019/9080279>.
- Duan, J., Yu, Y., Shi, H., Tian, L., Guo, C., Huang, P., Zhou, X., Peng, S., Sun, Z., Shah, V., 2013. Toxic effects of silica nanoparticles on Zebrafish embryos and larvae. *PLoS ONE* 8 (9). <https://doi.org/10.1371/journal.pone.0074606>.
- Ettxeberria, U., Garza, A.L., Campión, J., Martínez, J.A., Milagro, F.I., 2012. Antidiabetic effects of natural plant extracts via inhibition of carbohydrate hydrolysis enzymes with emphasis on pancreatic alpha amylase. *Expert Opin Ther Targets*. 16, 269–297. <https://doi.org/10.1517/14728222.2012.664134>.
- Ganesan, S., Anaimalai Thirumurthi, N., Raghunath, A., Vijayakumar, S., Perumal, E., 2016. Acute and sub-lethal exposure to copper oxide nanoparticles causes oxidative stress and teratogenicity in zebrafish embryos. *J. Appl. Toxicol.* 36 (4), 554–567.
- Garcia, G.R., Noyes, P.D., Tanguay, R.L., 2016. Advancements in zebrafish applications for 21st century toxicology. *Pharmacol. Ther.* 161, 11–21. <https://doi.org/10.1016/j.pharmthera.2016.03.009>.
- Gnanasundaram, I., Balakrishnan, K., 2017. Synthesis and evaluation of anti-inflammatory activity of silver nanoparticles from *Cissus vitifolia* leaf extract. *J. Nanosci. Tech.* 3, 266–269.
- Gunathilake, K.D.P.P., Ranaweera, K.K.D.S., Rupasinghe, H.P.V., 2018. Influence of boiling, steaming and frying of selected leafy vegetables on the *in vitro* anti-inflammation associated biological activities. *Plants* 7, 22. <https://doi.org/10.3390/plants7010022>.
- Jain, S., Mehata, M.S., 2017. Medicinal plant leaf extract and pure flavonoid mediated green synthesis of silver nanoparticles and their enhanced antibacterial property. *Sci. Rep.* 7, 15867. <https://doi.org/10.1038/s41598-017-15724-8>.
- Kumari, P., Panda, P.K., Jha, E., et al., 2017. Mechanistic insight to ROS and apoptosis regulated cytotoxicity inferred by green synthesized CuO nanoparticles from *Calotropis gigantea* to embryonic zebrafish. *Sci Rep.* 7, 16284. <https://doi.org/10.1038/s41598-017-16581-1>.
- Kuppasamy, P., Yusoff, M.M., Maniam, G.P., Govindan, N., 2016. Biosynthesis of metallic nanoparticles using plant derivatives and their new avenues in

- pharmacological applications-an updated report. *Saudi Pharm. J.* 24, 473–484. <https://doi.org/10.1016/j.jsps.2014.11.013>.
- Mamun, R.M., Akhter, K.N., Chowdhury, J.A., et al., 2017. Characterization of phytoconstituents and evaluation of antimicrobial activity of silver-extract nanoparticles synthesized from *Momordica charantia* fruit extract. *BMC Complement Altern. Med.* 17, 1–7. <https://doi.org/10.1186/s12906-016-1505-2>.
- Morikawa, T., Ninomiya, K., Tanabe, G., Matsuda, H., Yoshikawa, M., Muraoka, O., 2021. A review of antidiabetic active thiosugar sulfoniums, salacinol and neokotalanol, from plants of the genus *Salacia*. *J. Nat. Med.* 75, 449–466. <https://doi.org/10.1007/s11418-021-01522-0>.
- Mulvaney, P., 1996. Surface plasmon spectroscopy of nano sized metal particles. *Langmuir* 12, 788–800. <https://doi.org/10.1021/la9502711>.
- Nagabhushana, H., Basavaraj, R.B., Daruka Prasad, B., Sharma, S.C., Premkumar, H.B., Udayabhanu, , Vijayakumar, G.R., 2016. Facile, ECG., assisted green synthesis of raspberry shaped CdO nanoparticles. *J. Alloys Compd.* 669, 232–239.
- Nasrullah, M., Gul, F.Z., Hanif, S., Mannan, A., Naz, S., Ali, J.S., Zia, M., 2020. Green and chemical syntheses of CdO NPs: A comparative study for yield attributes, biological characteristics, and toxicity concerns. *ACS Omega* 5 (11), 5739–5747. <https://doi.org/10.1021/acsomega.9b03769>.
- Noorjahan, C.M., Jasmine Shahina, S.K., Deepika, T., Summera, R., 2015. Green Synthesis and Characterization of Zinc Oxide Nanoparticles from *Neem* (*Azadirachta indica*). *IJSETR*, 5751–5753.
- Permana, Y.N., Yulizar, Y., 2017. Potency of *Parkia speciosa* Hassk seed extract for green synthesis of CdO nanoparticles its characterization. *IOP Conf. Ser. Mater. Sci. Eng.* 188, <https://doi.org/10.1088/1757-899X/188/1/012018>.
- Prabakaran, A.S., Mani, N., 2019. Anti-inflammatory activity of silver nanoparticles synthesized from *Eichhornia crassipes*: An in vitro study. *J. Pharmacogn. Phytochem* 8, 2556–2558.
- Rautela, A., Rani, J., Debnath, M., 2019. Green synthesis of silver nanoparticles from *Tectona grandis* seeds extract: characterization and mechanism of antimicrobial action on different microorganisms. *J. Anal. Sci. Technol.* 10, 5. <https://doi.org/10.1186/s40543-018-0163-z>.
- Rokade, A.A., Patil, P., Seong, I.Y., Won, K.L., Seong, S.P., 2016. Pure green chemical approach for synthesis of Ag2O nanoparticles. *Green Chem. Lett. Rev.* 9, 216–222. <https://doi.org/10.1080/17518253.2016.1234005>.
- Schulte, C., Nagel, R., 1994. Testing acute toxicity in the embryo of zebrafish, *Brachydanio rerio*, as an alternative to the acute fish test: Preliminary results. *ALTA*. 22, 12–19. <https://doi.org/10.1177/026119299402200104>.
- Shah, K., Lu, Y., 2018. Morphology, large scale synthesis and building applications of copper nanomaterials. *Constr. Build. Mater.* 180, 544–578. <https://doi.org/10.1016/j.conbuildmat.2018.05.159>.
- Siddiqui, M.A., Ahmad, J., Al-Khedhairi, A.A., Musarrat, J., Alhadlaq, H.A., Ahamed, M., 2013. Copper oxide nanoparticles induced mitochondria mediated apoptosis in human hepatocellular carcinoma cells. *PLoS ONE* 8 (8), e69534. <https://doi.org/10.1371/journal.pone.0069534>.
- Sukumar, S., Rudrasenan, A., Nambiar, D.P., 2020. Green-Synthesized Rice-Shaped Copper Oxide Nanoparticles Using *Caesalpinia bonducella* Seed Extract and Their Applications. *ACS Omega*. 5, 1040–1051. <https://doi.org/10.1021/acsomega.9b02857>.
- Upadhyay, P.K., Jain, V.K., Sharma, S., Shrivastav, A.K., Sharma, R., 2020. Green and chemically synthesized ZnO nanoparticles: A comparative study. *IOP Conference Series: Mat. Sci. Eng.* 798 (1). <https://doi.org/10.1088/1757-899X/798/1/012025>.
- Yoshino, K., Miyauchi, Y., Kanetaka, T., Takagi, Y., Koga, K., 2009. Anti-diabetic activity of a leaf extract prepared from *Salacia reticulata* in mice. *Biosci. Biotechnol. Biochem.* 73, 1096–1104. <https://doi.org/10.1271/bbb.80854>.
- Zhu, X., Zhu, L., Duan, Z., Qi, R., Li, Y., Lang, Y., 2008. Comparative toxicity of several metal oxide nanoparticle aqueous suspensions to Zebrafish (*Danio rerio*) early developmental stage. *J Environ Sci Health A Tox Haz Subst Environ (Eng)* 43, 278–284. <https://doi.org/10.1080/10934520701792779>.